

1 **Increased inorganic aerosol fraction contributes to air pollution and**
2 **haze in China**

Yonghong Wang^{1,2}, Yuesi Wang^{1,6,8}, Lili Wang¹, Tuukka Petäjä^{2,3}, Qiaozhi
Zha², Chongshui Gong^{1,4}, Sixuan Li⁷, Yuepeng Pan¹, Bo Hu¹, Jinyuan Xin¹ and
Markku Kulmala^{2,3,5}

3 ¹State Key Laboratory of Atmospheric Boundary Layer Physics and Atmospheric Chemistry
4 (LAPC), Institute of Atmospheric Physics, Chinese Academy of Sciences, Beijing 100029,
5 China

6 ²Institute for Atmospheric and Earth System Research / Physics, Faculty of Science, P.O.Box
7 64, 00014 University of Helsinki, Helsinki, Finland

8 ³Joint international research Laboratory of Atmospheric and Earth SysTem sciences
9 (JirLATEST), Nanjing University, Nanjing, China

10 ⁴Institute of Arid meteorology, China Meteorological Administration, Lanzhou 730000,
11 China

12 ⁵Aerosol and Haze Laboratory, Beijing Advanced Innovation Center for Soft Matter Science
13 and Engineering, Beijing University of Chemical Technology (BUCT), Beijing, China

14 ⁶Centre for Excellence in Atmospheric Urban Environment, Institute of Urban Environment,
15 Chinese Academy of Science, Xiamen, Fujian 361021, China

16 ⁷State Key Laboratory of Numerical Modeling for Atmospheric Sciences and Geophysical
17 Fluid Dynamics (LASG), Institute of Atmospheric Physics, Chinese Academy of Sciences,
18 Beijing 100029, China

19 ⁸University of Chinese Academy of Sciences, Beijing 100049, China

20 Revised to: Atmospheric Chemistry and Physics

21 Corresponding authors: Y.S. Wang, L.L.Wang and M. Kulmala

22 E-mail: wys@mail.iap.ac.cn; wll@mail.iap.ac.cn; markku.kulmala@helsinki.fi

23 **Abstract**

24 The detailed formation mechanism of increased number of haze events in China is
25 still not very clear. Here, we found that reduced surface visibility from 1980-2010 and
26 an increase in satellite derived columnar concentrations of inorganic precursor from
27 2002 to 2012 are connected with each other. Typically higher inorganic mass fractions
28 lead to increased aerosol water uptake and light scattering ability in elevated relative
29 humidity. Satellite observation of aerosol precursors of NO₂ and SO₂ showed increased
30 concentrations during study period. Our in-situ measurement of aerosol chemical
31 composition in Beijing also confirmed increased contribution of inorganic aerosol
32 fraction as a function of increased particle pollution level. Our investigations
33 demonstrate that the increased inorganic fraction in the aerosol particles is a key
34 component in the frequently occurring haze days during studying period, and
35 particularly the reduction of nitrate, sulfate and their precursor gases would contribute
36 towards better visibility in China.

37 **Introduction**

38 As one of the most heavily polluted regions in the world, China has suffered from
39 air pollution for decades (Hao et al., 2007; Zhang et al., 2015). Aerosol particles, as
40 major air pollutant, have significant effects on human health (Lelieveld et al., 2015).
41 The general public and the central government of China have realized the severe
42 situation and have taken some actions to improve the air quality nationwide in the recent
43 years. For example, the state council published a plan for air pollution control, in

44 September of 2013, aim to reduce PM_{2.5} concentrations by 10%~25% in different
45 regions of China. The successful implementation requires a sufficient knowledge of
46 haze formation mechanism (Kulmala, 2015) and comprehensive observation network
47 (Kulmala, 2018). Our understanding on haze events with high PM_{2.5} concentrations in
48 China is still limited due to the spatial-temporal variation of aerosol properties and
49 limited observation information (Wang et al., 2016). Recent studies found that
50 secondary aerosol components are important during the intense haze events in Beijing,
51 Xi'an, Chengdu and Guangzhou during January of 2013, and the reduction of aerosol
52 precursors is a key step to reduce particle pollution (Guo et al., 2014; Huang et al.,
53 2014). The analysis of longer time series data from Nanjing shows that secondary
54 particles are typically dominating even the number concentrations in polluted
55 conditions (Kulmala ., 2016). [A recent study have suggested significantly decreased](#)
56 [trends of PM_{2.5} and SO₂ in China from 2015-2017 by analyzing data sets from Ministry](#)
57 [of Ecology and Environment of China \(Silver et al., 2018\). The column NO₂](#)
58 [concentration obtained from OMI showed increased trend during 2005-2011, while a](#)
59 [decreasing trend during 2012-2015 \(Itahashi et al., 2016\). The SO₂ concentration has](#)
60 [decreased around 50% from 2012-2015 in North China Plain due to economic](#)
61 [slowdown and governments efforts to restrain emissions from power and industrial](#)
62 [sectors \(Krotkov et al., 2016\). However, the most abundant mass fractions of](#)
63 atmospheric aerosol are inorganic and organic components, which have large spatio-
64 temporal variation (Jimenez et al., 2009). Identifying the most abundant as well as
65 critical aerosol species that contribute to the haze formation in a longtime perspective
66 is important to draw up effective plans for the air pollution control.

67 Here, a comprehensive data sets were used to reveal that an increasing trend of
68 inorganic components in atmospheric aerosol may be a pivotal factor, at least, which

69 leads to frequently occurred haze events in China from 1980-2010. We suggests that
70 the controlling of inorganic aerosol components of nitrate, sulfate and their precursors
71 should be of a high priority due to their strong water uptake abilities and therefore, light
72 scattering ability in high RH conditions.

73 **2.Methodology**

74 The daily averaged visibility and relative humidity data in 262 sites of China are
75 obtained from the Integrated Surface Dataset (ISD) from National Oceanic and
76 Atmospheric Administration National Climate Data Center of the USA from 1980-
77 2010 (<https://www.ncdc.noaa.gov/isd>). The visibility observations were made three
78 times a day at 8-hour intervals begins at 00:00 by well trained technicians. They
79 measured visual range using distinctive markers, such as tall buildings, mountains and
80 towers, to which the distance from the meteorological monitoring stations are known.

81 We quantified the importance of relative humidity to visibility as the hygroscopic
82 inorganic compounds typically grow in size in high humidity (Swietlicki et al., 2008).
83 Aerosol size growth and composition change in high humidity condition are highly
84 related light scattering ability (Zhang et al., 2015). Studies always use $f(RH)$, a
85 parameter which is defined as the ratio of light scattering coefficient under high RH
86 with that under low RH. $f(RH)$ is a unitless number, usually ranges from one to two.
87 At ambient RH around 80%, a higher $f(RH)$ value usually corespondes to higher
88 inorganic aerosol fraction, while a lower value usually corespondes to high organic
89 fraction. The reason is that inorganic aerosol compounds of nitrate,sulfate and
90 ammonium have more strong water uptake ability than organic comopounds. In
91 addition, the high humidity condition in ambient prefers the formation of inroganici
92 aerosol from precursors of NO_2 and SO_2 (Wang et al., 2014). In this study, for a given

93 site and given year, we defined a f (RH)-like parameter, R_i , using the observed annual
94 visibility (V) as a ratio (R_i) between visibility values from the surface observation
95 stations, when the daily average RH was below 40% for more than 20 days. In the
96 corresponding high-humidity cases daily RH was between 80%~90% for more than
97 20 days each year at a given observation site:

98

$$99 \quad R_i = \frac{V_{dry}}{V_{wet}}.$$

100 We use this ratio to infer long trend of aerosol hygroscopicity information. In
101 addition, we calculate anomaly (A) from the ratio for a given year i as a difference from
102 the 30-year (R_{30y}) from 1980 to 2010:

$$103 \quad A = R_i - R_{30y}.$$

104 Our spatial focus is placed on North China Plain, Yangtze River Plain and Sichuan
105 Basin due to frequent haze events (Zhang et al., 2012). The stations in Pearl River delta
106 region and other Southern China stations were not included due to limited days with
107 the daily average RH below 40%.

108 The atmospheric column amount of NO_2 and SO_2 data are obtained from 2002-2012
109 and 2004-2012, respectively, from SCIAMACHY (Scanning Imaging Absorption
110 spectrometer for Atmospheric CHartography) satellite products. SCIAMACHY is an
111 atmospheric sensor aboard the European satellite ENVISAT. It was launched in March 2002 as
112 a joint project of Germany, the Netherlands and Belgium. It measures atmospheric absorption
113 in spectral bands from the ultraviolet to the near infrared (240 nm - 2380 nm), allows to retrieve
114 atmospheric column concentrations of O_3 , BrO, OClO, ClO, SO_2 , H_2CO , NO, NO_2 , NO_3 , CO,
115 CO_2 , CH_4 , H_2O , N_2O , aerosols, radiation and cloud properties (Boersma et al., 2004) . Aerosol

116 chemical composition from GEOS (Goddard Earth Observing System)-Chem chemical
117 transport model combined with satellite AOD products in China during 1998-2012 is
118 used. The model utilizes assimilated meteorology data and regional emission
119 inventories with a horizontal resolution of $2^{\circ}\times 2^{\circ}$ with 47 vertical levels from surface to
120 80 km. The $PM_{2.5}$ concentration was retrieved from AOD of satellite and the
121 relationship between $PM_{2.5}$ and AOD in GEOS-Chem. The detailed information about
122 the model can be found in (Boys et al., 2014). Aerosol chemical composition of organic,
123 sulfate, nitrate, ammonium and chloride were measured with a high-resolution-time of
124 flight-aerosol mass spectrometers during an intensive campaign in urban Beijing from
125 November of 2010 to January of 2011 (DeCarlo et al., 2006). Detailed information of
126 data analysis, collection efficiencies (CE) and relative ionization efficiencies are
127 presented in Zhang et al. (2014).

128 **3. Results and discussion**

129 **3.1 Decreasing trend in visibility in high relative humidity conditions**

130 According to the geographical division, our study sites are mainly in North China
131 Plain (NCP), Sichuan Basin (SCB) and Yangtze River Plain (YRP) as showed in Figure
132 1. The average visibility in low RH in NCP, SCB, YRP and China are 18.2 km, 21.4
133 km, 19.5 km and 23.3 km, while the values in high RH conditions are 10.6 km, 13.7
134 km, 13.7 km and 17.4 km, respectively. In general, visibility in low RH condition has
135 fluctuated trend, particularly in Northern China Plain, Sichuan Basin and Yangtze river
136 Plain region, whereas visibility in high RH conditions showed decreasing trend as
137 shown in Figure S1 (a) and (b) . The average ratio of visibility in low RH to that in high
138 RH from 1980-2010 is presented in Figure 1. The maximum ratios were identified in
139 eastern China and in some western Chinese cities. Three heavily polluted regions,

140 Northern China Plain, Sichuan Basin and Yangtze river Plain were identified based on
141 values of high R_i , which are also constant with aerosol mass concentrations and haze
142 day distributions (van Donkelaar et al., 2010; Xin et al., 2015). That is, the higher ratios
143 occurred in more severe air pollution areas, like North China Plain, Sichuan Basin and
144 the city of Urumqi, where the contribution of hygroscopic aerosol is more pronounced
145 in comparison with non-hygroscopic dust particles. The average R_i during 1980-1984
146 in Northern China Plain, Sichuan Basin and Yangtze river Plain are 1.62, 1.41, 1.29
147 and 1.31, respectively, contrasting with the values of 1.98, 1.81, 1.70 and 1.52 during
148 2006-2010. The increments are 22.3%, 27.3%, 31% and 16%, respectively. It is worth
149 noting that the R_i in Yangtze river Plain region exhibits the most increment, which
150 implies the increased emissions with rapid economic growth. Long time trends of this
151 ratio in a specific site can reveal the variation of aerosol inorganic fraction and organic
152 fraction due to their different hygroscopicity and water uptake capacity and associated
153 light extinction ability. That is, the mass fractions and concentrations of sulfate, nitrate
154 and ammonium may have increased over study period as they dominate water uptake
155 ability compared with other components (e.g., organic, black carbon, dust and metal
156 elements, see Table S1) in the atmospheric aerosol (Wang et al., 2015). For the selected
157 regions, we have calculated the anomaly as a regional average as shown in Figure 2.
158 The ratio showed increasing trends over three regions of China and the maximum trends
159 occurred in North China Plain with the value of 0.0168 per year, which indicate an
160 increase of hygroscopic aerosol in these regions during the 30-year observation period.

161 To corroborate our results, Yang et al. (2011) showed an increasing fraction of
162 inorganic components by 20% in Beijing from 1998 to 2008 using in-situ offline [aerosol](#)
163 [chemical composition](#) measurement, especially in summer, while the fractions of
164 hydrophobic components such as organic and black carbon decreased in the aerosol

165 phase. A study by Boys et al. (2014) revealed that increasing fraction of secondary
166 inorganic aerosol is dominated in the increased mass concentration of PM_{2.5} in China
167 from 1998-2012 using GEOS-Chem model [combined satellite results](#). By using
168 observed meteorology data sets, Fu et al. (2014) revealed that the number of haze days
169 have significantly increased in the past three decades over North China Plain due to the
170 increase in hygroscopic inorganic aerosol composition.

171 **3.2 Enhanced emissions of inorganic aerosol precursors**

172 The longterm trends of aerosol precursors and their spatial variability can improve
173 our understanding of the trends in aerosol chemical composition. Figure 3 and Figure
174 4 show atmospheric column trends of NO₂ and SO₂ observed from SCIAMACHY. The
175 column NO₂ level can be a good proxy for vehicle and coal burning emission associated
176 with oil and coal consumption (Richter et al., 2005). The column amount of NO₂
177 showed pronounced increasing trends in three regions of China, particularly in Northern
178 China with the value of 0.14×10^{15} molecule/cm²/year from 2002 to 2011. This is
179 probably associated with the increase in power plant and on-road vehicle emissions
180 [\(Wu et al., 2012; Krotkov et al., 2016\)](#). The average NO₂ concentration in Northern
181 China increased by more than two-fold, while in the Yangze River Plain region
182 experienced a considerable smaller trend in NO₂, with the value of 9.7×10^{15}
183 molecule/cm² in 2010 and 6.4×10^{15} molecule/cm² in 2002. [It is worth noting a](#)
184 [decreased trend occurred during year 2008, which is mainly due to emission reduction](#)
185 [during the Olympic games and economic downturn \(Lin and McElroy, 2011\)](#). As a
186 whole, the column NO₂ concentration in China doubled from 2002 to 2010, with the
187 values of 1.4×10^{15} molecule/cm² in 2002 and 2.8×10^{15} molecule/cm² in 2010,
188 respectively.

189 Figure 4 depicts trend in SO₂ concentration in four regions of China from 2004 to
190 2010. The SO₂ concentration showed an increasing trends in North China Plain,
191 Sichuan Basin and Yangze River Plain, but increased mostly in China from 2004 to
192 2012. A decreasing trend was observed during the year of 2008 and 2009, especially in
193 Northern China Plain. This may be due to a combination of Chinese economic
194 downturn and emission reduction during the Olympic games (Lin and McElroy, 2011)
195 (Wang et al., 2010). Anyway, as an important aerosol precursor, NO₂ showed the
196 most increasing trend in China from 2002-2012 , consistent with the trend of increased
197 aerosol concentration by modeling result (Xing et al., 2015). Figure S3 shows the
198 annual trends of aerosol inorganic fraction in PM_{2.5} mass concentration from 1998-2012
199 with GEOS-Chem model combined with satellite results in China. The results indicate
200 that North China Plain area suffered the most from heavily pollution, consistent with
201 our surface observations (Xin et al., 2015). Aerosol concentrations have increased
202 considerably from 1980 to 2010. The modeling combined with satellite results by Boys et al.
203 (2014) show that concurrently the fraction of inorganic fraction has increased more rapidly.
204 Consequently, the water uptake of the aerosol have increased leading to reduced visibility as
205 we suggested, which is consistent with ground-based observations (Yang et al., 2011).

206 **3.3 Validation of increased inorganic aerosol components with elevated air** 207 **pollution level with in-situ measurement**

208 To validate our hypothesis that the increased inorganic components contribute to
209 visibility degradation, we used four months of aerosol chemical composition and
210 visibility data from urban Beijing from November of 2010 to February of 2011. As
211 shown in Figure 5, we divided the visibility values into four bins, which corresponds to
212 clean time to heavy pollution time and to conditions in between. The inorganic aerosol

213 precursors of SO₂ and NO₂ nearly doubled as the visibility decreased from more than
214 10 km (clean time) to less than 2 km (heavily polluted time). At the same time, the mass
215 concentrations of nitrate, sulfate and ammonium components increased to 13.5 µg m⁻³,
216 15.5 µg m⁻³ and 10.6 µg m⁻³, respectively. Meanwhile, the mass fraction of these
217 inorganics increased from 11.3% to 17.3%, from 13.0% to 19.9% and from 9.6% to
218 13.6%, respectively. At the same time, the mass concentration and fraction of organic
219 components changed from 12.2 µg m⁻³ to 33.4 µg m⁻³ and 60% to 46%, respectively.

220 We also investigated the relationship between relative humidity (RH) and volume
221 fractions of ammonium sulfate, ammonium nitrate and organic aerosols as shown in Figure 6.
222 The results indicated that ammonium nitrate increased most significantly with elevated RH. On
223 the contrary, ammonium sulfate, as another inorganic compound, showed only a moderate
224 positive correlation with RH and a decrease in the volume fraction was observed in RH values
225 larger than 75%. This might be associated with liquid phase oxidation of SO₂ under high RH
226 condition, to sulfate aerosol. Increasing RH may provide more atmospheric oxidants and
227 reaction media for the aqueous-phase oxidation (Zhang et al., 2015). The volume fraction of
228 organic aerosol showed negative correlation with increasing RH, as presented in Figure 6 (c),
229 which was maybe due to a faster increasing volume fraction of inorganic aerosol than organic
230 aerosol.

231 This direct observation shows that the contribution of inorganic components increased
232 during this campaign. It is plausible that the increased concentration of SO₂ and NO₂
233 are highly associated with this giving rise to the long-term trends observed in Figure 2
234 (Pan et al., 2016; Wang et al., 2014).

235 **4. Conclusion and implication for atmospheric air pollution control**

236 Atmospheric pollution and associated haze events has a dramatic effect on climate
237 change, human health and visibility degradation (Ding et al., 2013; Petäjä et al., 2016;

238 Wang et al., 2015; Zhang et al., 2015). Here, longterm visibility measurements
239 combined with satellite data sets, in-situ measurements and model results revealed that
240 increased fractions of inorganic aerosol components in the particle matter are crucial in
241 contributing to more haze events [from 1980-2010](#). In this way, aerosol hygroscopic
242 growth has occurred in lower relative humidity conditions than before due to more
243 ammonium nitrate aerosol, and the light scattering ability of atmospheric aerosol
244 enhanced as shown in Figure 7. Another mechanism is that high concentration of NO_x
245 can promote the conversion of SO₂ to form sulfate aerosol via aqueous phase oxidation
246 during intensive pollution periods (He et al., 2014; Wang et al., 2016). Considering the
247 vast energy consumption in the future decades and the sources of inorganic components
248 in atmospheric aerosol, we demonstrate that the reduction nitrate, sulfate, ammonium
249 and their precursors [should be continued to get better visibility](#) in China.

250

251 Acknowledgements

252 We acknowledge Dr B. Boys and Professor R. Martin of Dalhousie University for providing
253 GEOS-Chem model results in China. We acknowledge the free use of tropospheric NO₂ and SO₂
254 column data from the SCIAMACHY sensor from www.temis.nl. This work was supported by the
255 Ministry of Science and Technology of China (No: 2017YFC0210000), the National Research
256 Program for key issues in air pollution control (DQGG0101), the National Natural Science
257 Foundation of China No.41775162 and Academy of Finland via Center of Excellence in
258 Atmospheric Sciences and the National Natural Science Foundation of China (41605119).

259

260 **Competing financial interests**

261 The authors declare no competing financial interests.

262 **Author contributions**

263 Y.H.W had the original idea. L.L.W and C.S.G provided and processed satellite and

264 visibility data. Y.S.W provided measurements of aerosol chemical composition

265 data. Y.H.W, Y.S.W, L.L.W, T.P and M.K interpreted the data and write the paper.

266 All the authors commented on the paper.

267 **References**

268 Boersma, K. F., Eskes, H. J. and Brinksma, E. J.: Error analysis for tropospheric NO₂ retrieval

269 from space, *Journal of Geophysical Research: Atmospheres*, 109(D4), n/a-n/a,

270 doi:10.1029/2003jd003962, 2004.

271 Boys, B.L. et al. Fifteen-Year Global Time Series of Satellite-Derived Fine Particulate Matter.

272 *Environmental Science & Technology*, 48(19): 11109-11118, 2014.

273 DeCarlo, P.F. et al. Field-Deployable, High-Resolution, Time-of-Flight Aerosol Mass

274 Spectrometer. *Analytical Chemistry*, 78(24): 8281-8289, 2006.

275 Ding, A.J. et al.. Intense atmospheric pollution modifies weather: a case of mixed biomass burning

276 with fossil fuel combustion pollution in eastern China. *Atmos. Chem. Phys.*, 13(20):

277 10545-10554, 2013.

278 Fu, G.Q., Xu, W.Y., Yang, R.F., Li, J.B. and Zhao, C.S. The distribution and trends of fog and

279 haze in the North China Plain over the past 30 years. *Atmos. Chem. Phys.*, 14(21): 11949-

280 11958, 2014.

281 Guo, S. et al. Elucidating severe urban haze formation in China. *Proceedings of the National*

282 *Academy of Sciences of the United States of America*, 111(49): 17373-8, 2014.

283 Hao, J., He, K., Duan, L., Li, J. and Wang, L. Air pollution and its control in China. *Frontiers of*

284 *Environmental Science & Engineering in China*, 1(2): 129-142, 2007

285 He, H. et al. Mineral dust and NO_x promote the conversion of SO₂ to sulfate in heavy pollution
286 days. *Sci Rep*, 4: 4172, 2014.

287 Huang, R.J. et al. High secondary aerosol contribution to particulate pollution during haze events
288 in China. *Nature*, 514(7521): 218-22, 2014.

289 Itahashi, S., Muto, T., Irie, H., Uno, I. and Kurokawa, J.: Turnaround of Tropospheric Nitrogen
290 Dioxide Pollution Trends in China, Japan, and South Korea, *Sola*, 12(0), 170–174,
291 doi:10.2151/sola.2016-035, 2016.

292 Jimenez, J.L. et al. Evolution of Organic Aerosols in the Atmosphere. *Science*, 326(5959): 1525-
293 1529, 2009.

294 Krotkov, N. A., McLinden, C. A., Li, C., Lamsal, L. N., Celarier, E. A., Marchenko, S. V.,
295 Swartz, W. H., Bucsela, E. J., Joiner, J., Duncan, B. N., Boersma, K. F., Veefkind, J. P.,
296 Levelt, P. F., Fioletov, V. E., Dickerson, R. R., He, H., Lu, Z. and Streets, D. G.: Aura
297 OMI observations of regional SO₂ and
298 NO₂ pollution changes from 2005 to 2015,
299 *Atmospheric Chemistry and Physics*, 16(7), 4605–4629, doi:10.5194/acp-16-4605-2016,
300 2016

301 Kulmala, M.. Build a global Earth observatory. *Nature*, 553, 2018.

302 Kulmala, M.. China's choking cocktail. *Nature*, 526, 2015.

303 Kulmala M., L.K., Virkkula A., Petäjä T., Paasonen P., Kerminen V.-M., Nie W., Qi X., Shen Y.,
304 Chi X. & Ding A. On the mode-segregated aerosol particle number concentration load:
305 contributions of primary and secondary particles in Hyytiälä and Nanjing. *Boreal Env.*
306 *Res*, 21: 319–331, 2016.

307 Lelieveld, J., Evans, J.S., Fnais, M., Giannadaki, D. and Pozzer, A. The contribution of outdoor air
308 pollution sources to premature mortality on a global scale. *Nature*, 525(7569): 367-71,
309 2015.

310 Lin, J.T. and McElroy, M.B. Detection from space of a reduction in anthropogenic emissions of
311 nitrogen oxides during the Chinese economic downturn. *Atmos. Chem. Phys.*, 11(15):
312 8171-8188, 2011.

313 Pan, Y. et al. Redefining the importance of nitrate during haze pollution to help optimize an
314 emission control strategy. *Atmospheric Environment*, 141: 197-202, 2016.

315 Peng, J. et al. Markedly enhanced absorption and direct radiative forcing of black carbon under
316 polluted urban environments. *Proceedings of the National Academy of Sciences*, 113(16):
317 4266-4271, 2016.

318 Petäjä, T. et al. Enhanced air pollution via aerosol-boundary layer feedback in China. *Scientific*
319 *Reports*, 6: 18998, 2016.

320 Richter, A., Burrows, J.P., Nusz, H., Granier, C. and Niemeier, U. Increase in tropospheric
321 nitrogen dioxide over China observed from space. *Nature*, 437(7055): 129-132, 2005.

322 Swietlicki, E. et al. Hygroscopic properties of submicrometer atmospheric aerosol particles
323 measured with H-TDMA instruments in various environments—a review. *Tellus B:*
324 *Chemical and Physical Meteorology*, 60(3): 432-469, 2008.

325 van Donkelaar, A. et al. Global estimates of ambient fine particulate matter concentrations from
326 satellite-based aerosol optical depth: development and application. *Environmental health*
327 *perspectives*, 118(6): 847-855, 2010.

328 Wang, G. et al. Persistent sulfate formation from London Fog to Chinese haze. *Proceedings of the*
329 *National Academy of Sciences*, 113(48): 13630-13635, 2016.

330 Wang, S. et al. Quantifying the Air Pollutants Emission Reduction during the 2008 Olympic
331 Games in Beijing. *Environmental Science & Technology*, 44(7): 2490-2496, 2010.

332 Wang, Y. et al. Mechanism for the formation of the January 2013 heavy haze pollution episode
333 over central and eastern China. *Science China Earth Sciences*, 57(1): 14-25, 2014.

334 Wang, Y.H. et al. Aerosol physicochemical properties and implications for visibility during an
335 intense haze episode during winter in Beijing. *Atmos. Chem. Phys.*, 15(6): 3205-3215,
336 2015.

337 Wu, Y. et al. The challenge to NO_x emission control for heavy-duty diesel vehicles in China.
338 *Atmos. Chem. Phys.*, 12(19): 9365-9379, 2012.

339 Xin, J. et al. The Campaign on Atmospheric Aerosol Research Network of China: CARE-China.
340 *Bulletin of the American Meteorological Society*, 96(7): 1137-1155. 2015.

341 Xing, J. et al. Observations and modeling of air quality trends over 1990–2010 across the Northern
342 Hemisphere: China, the United States and Europe. *Atmos. Chem. Phys.*, 15(5): 2723-
343 2747, 2015.

344 Yang, F. et al. Characteristics of PM_{2.5} speciation in representative megacities and across China.
345 *Atmos. Chem. Phys.*, 11(11): 5207-5219, 2011.

346 Zhang, J.K. et al. Characterization of submicron aerosols during a month of serious pollution in
347 Beijing, 2013. *Atmos. Chem. Phys.*, 14(6): 2887-2903, 2014.

348 Zhang, R. et al. Formation of urban fine particulate matter. *Chem Rev*, 115(10): 3803-55, 2015

349 Zhang, X.Y. et al. Atmospheric aerosol compositions in China: spatial/temporal variability,
350 chemical signature, regional haze distribution and comparisons with global aerosols.
351 *Atmos. Chem. Phys.*, 12(2): 779-799, 2012.

352

353

354

355

356

357

358

359

360

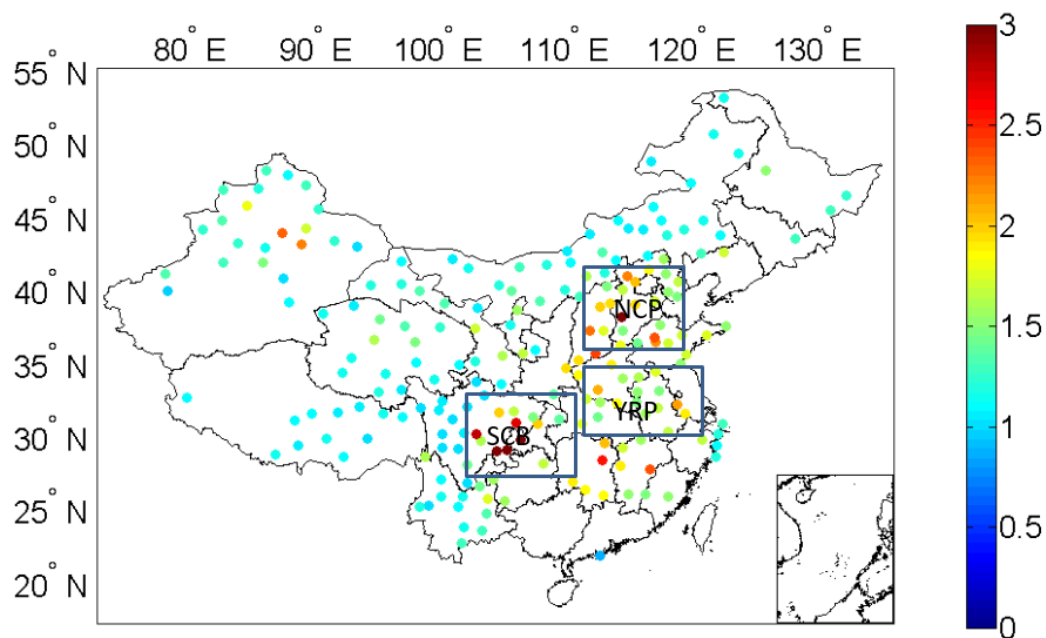
361

362

363

364

Figure caption



365

366 **Figure 1.** The distribution of the average surface visibility ratio in dry and wet
367 conditions based on observations at 262 surface observation sites in China. The
368 aerosol in the industrialized regions of China in the East are more hygroscopic than
369 aerosol particles in the west of China.

370

371

372

373

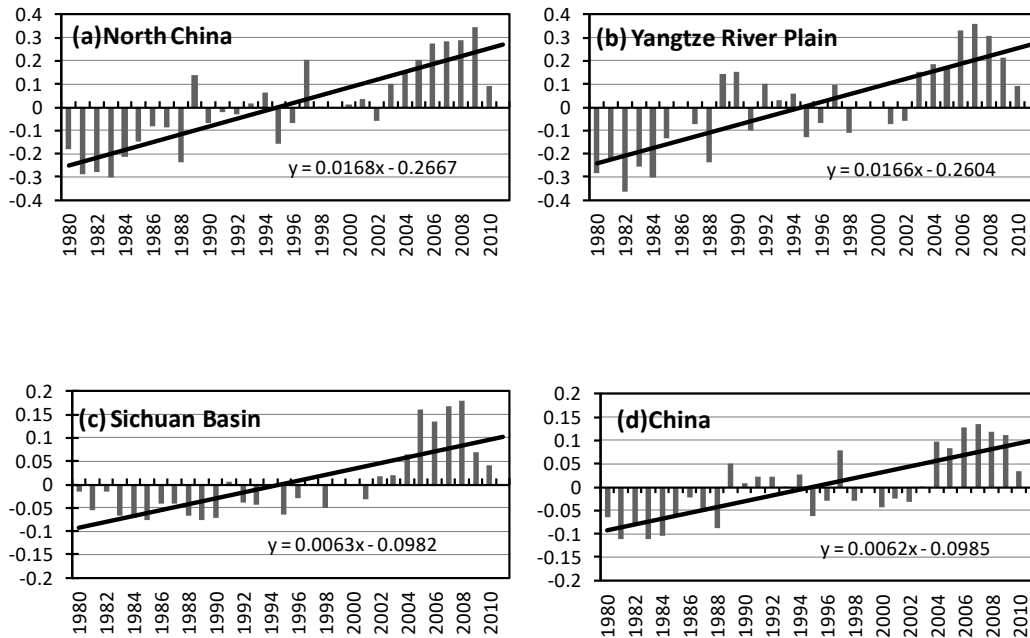
374

375

376

377

378



379

380 **Figure 2.** Anomalies and trends of ratio of visibility in North China Plain, Yangtze
381 Plain, Sichuan Basin and in China as a whole. The relative contribution of
382 hygroscopic aerosols to the visibility reduction has increased from 1980 to 2010 in
383 China.

384

385

386

387

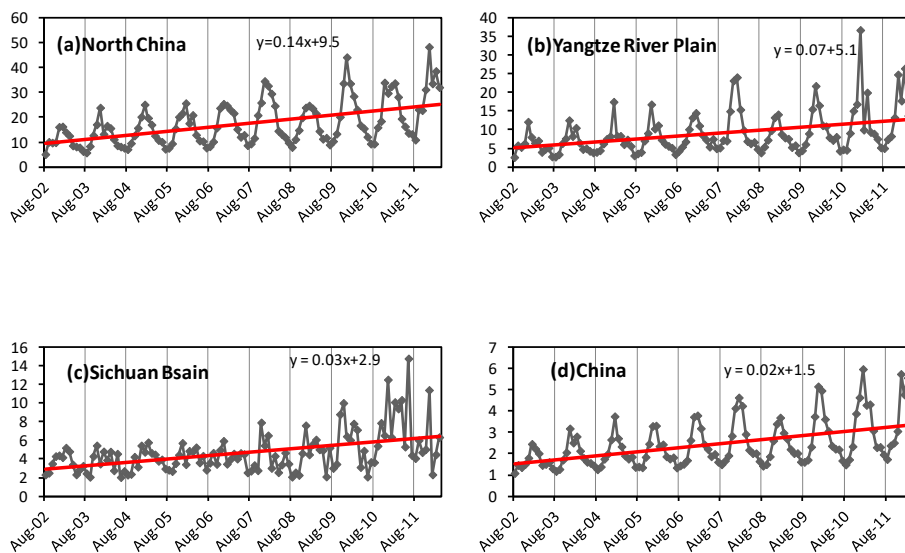
388

389

390

391

392



393

394

Figure 3. Trends of NO₂ concentration over china from SCIAMACHY from the year

395

2002 to 2012 (10¹⁵ mol/cm²)

396

397

398

399

400

401

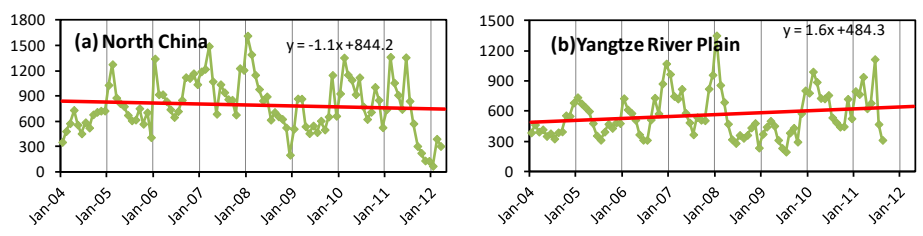
402

403

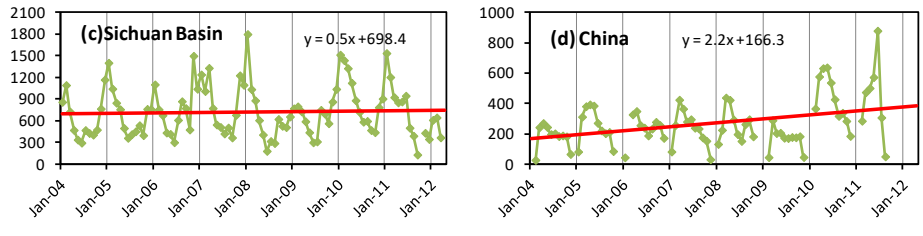
404

405

406



407



408

Figure 4. Trends of SO₂ concentration over china from SCIAMACHY from the year of

409

2004 to 2012 (1000DU)

410

411

412

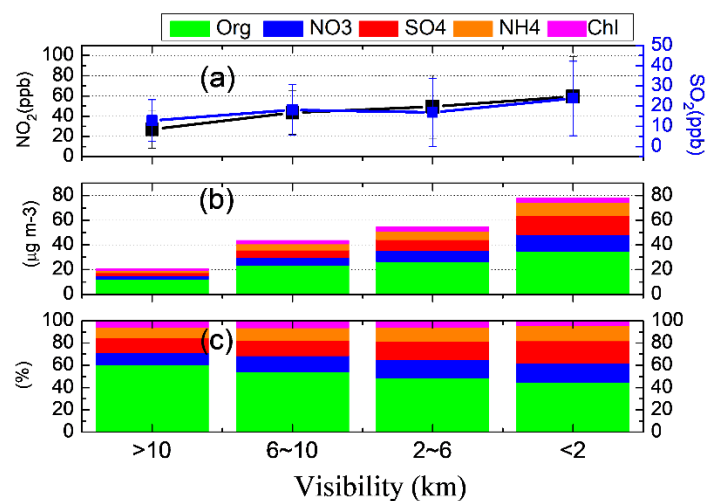
413

414

415

416

417



418

419

420

421

422 **Figure 5:** Variation of (a) NO₂, SO₂, (b) chemical composition (c) mass fraction of

423 organic, nitrate, sulfate, ammonium and chloride with decreased visibility during the

424 intensive campaign in Beijing.

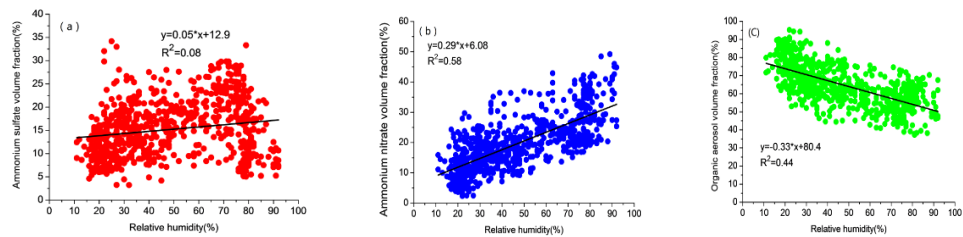
425

426

427

428

429



430

431 Figure 6. Relation between relative humidity (RH) and volume fractions of (a) ammonium

432 sulfate (b) ammonium nitrate (c) organic aerosol.

433

434

435

436

437

438

439

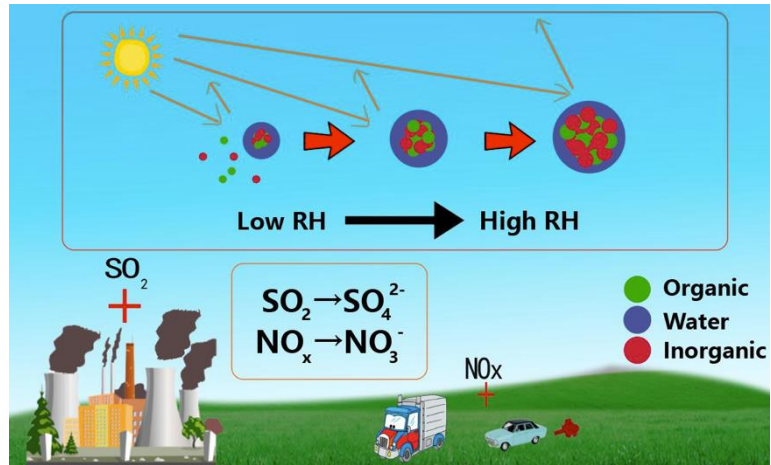
440

441

442

443

444



445

446 Figure 7. A schematic picture illustrating the process of enhanced emission of
 447 aerosol inorganic precursors and formation of aerosol inorganic components leading to
 448 increased hygroscopicity and aerosol water uptake ability leading to considerable
 449 visibility degradation in China. The plus symbols represents the strengthening of a
 450 specific process.

451

452